Fusion Engineering and Design 96–97 (2015) 136–141

Contents lists available at ScienceDirect

Fusion Engineering and Design

journal homepage: www.elsevier.com/locate/fusengdes

Development of a high-heat flux cooling element with potential application in a near-term fusion power plant divertor

Jack Robert Nicholas[a,*], Peter Ireland[a], David Hancock[b], Dan Robertson[c]

[a] Osney Thermo-Fluids Laboratory, University of Oxford, Oxford, United Kingdom
[b] CCFE, Culham, Oxfordshire, United Kingdom
[c] Rolls-Royce Plc., Derby, Derbyshire, United Kingdom

HIGHLIGHTS

- Laminate jet impingement system introduced for high pressure operation (17 MPa+).
- Numerical thermo-fluid analysis on baseline geometry.
- Cascade impingement shown to reduce divertor mass flow rate requirements and increase fluid temperature change.
- Numerical thermo-fluid analysis validated using scaled experiments with air.

ARTICLE INFO

Article history:
Received 4 October 2014
Received in revised form 10 March 2015
Accepted 12 March 2015
Available online 16 April 2015

Keywords:
Divertor
Water cooled
Jet impingement
High heat flux

ABSTRACT

A low temperature jet impingement based heat sink module has been developed for potential application in a near-term fusion power plant divertor. The design is composed of a number of hexagonal CuCrZr sheets bonded together in a stack to form a laminate structure. This method allows the production of complex flow paths using relatively simple manufacturing techniques. The thermo-fluid performance of a baseline design employing cascade jet impingement has been assessed and compared to a non-cascade case. Experimental validation of the numerical work was carried out on a scaled model using air as the working fluid. Local heat transfer coefficients were obtained on the surface using surface temperature data from thermochromic liquid crystals.

© 2015 The Authors. Published by Elsevier B.V. This is an open access article under the CC BY license (http://creativecommons.org/licenses/by/4.0/).

1. Introduction

A low temperature heat sink concept employing jet impingement has been developed for potential applications in a future fusion power plant. The design differs from other jet impingement approaches proposed in the literature [1–4] in its use of a cascading fluid flow path. Geometrically it is composed of a number of sheets stacked together and bonded in a laminate structure. By forming the geometry in this way complex three dimensional flow paths can be produced without compromising manufacturability.

For the structural material of the plates the alloy CuCrZr was chosen. This material offers the best heat flux handling capacity at the temperatures envisaged for operation and has been extensively researched in the fusion community. Due to the small 200–350 °C temperature window predicted for CuCrZr under DEMO relevant conditions [5] water is the preferred coolant for the design.

A baseline concept employing a hexagonal sheet structure has been developed and its thermo-fluid performance assessed using both numerical and experimental methods. The goal is the development of a heat sink capable of withstanding heat fluxes in the 10–20 MW/m^2 range whilst also maximizing the temperature change of the fluid.

2. Design features

2.1. Operational pressure

In current tokamak devices the heat flux handling capacity of the divertor has been of primary concern. As we move towards a fusion power plant maximizing the outlet temperature of the divertor also becomes important.

To achieve this with liquid water as the coolant we must increase the system pressure and reduce the mass flow rate requirements.

* Corresponding author. Tel.: +44 1865 288723.
E-mail address: jack.nicholas@eng.ox.ac.uk (J.R. Nicholas).

http://dx.doi.org/10.1016/j.fusengdes.2015.03.033
0920-3796/© 2015 The Authors. Published by Elsevier B.V. This is an open access article under the CC BY license (http://creativecommons.org/licenses/by/4.0/).

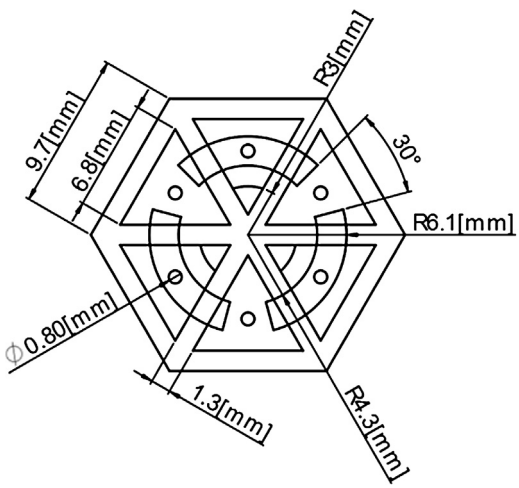

Fig. 1. Dimensions of baseline hexagonal heat sink concept.

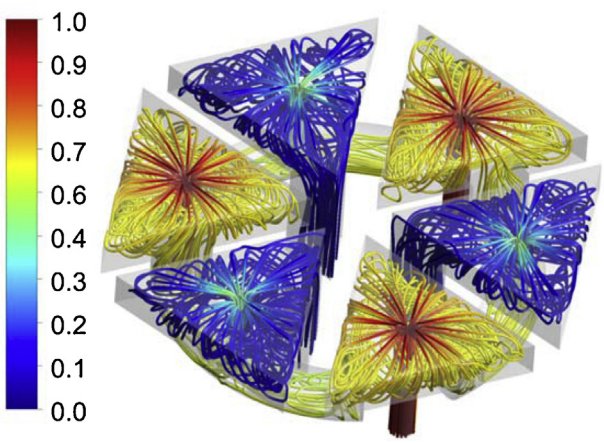

Fig. 2. Normalized total pressure drop through baseline fluid flow path.

In a closed divertor coolant loop peak temperature will also be limited by the heat sink material. For CuCrZr under DEMO relevant conditions this is approximately 350 °C [5]. Above 16.5 MPa the saturation temperature of water is greater than this value. Operating at pressures in excessive of 16.5 MPa means that peak fluid temperatures are limited structurally, rather than by the fluid. If a combined divertor to blanket coolant loop is utilized increasing the pressure further is beneficial.

To handle such pressures in a laminated sheet structure the hexagonal surface was divided into a number of triangular cavities. This was preferable over a multi-hexagonal structure as it limited stress concentration regions. A plan view of the baseline concept designed for a pressure of 20 MPa is depicted in Fig. 1.

2.2. Fluid flow-path

To cool the hexagonal surface a single impinging jet is employed in each of the triangular cavities. These are positioned at the centroid of the triangle. As the wall jet moves out from the stagnation region it eventually meets the cavity wall where a secondary impingement occurs.

A streamline plot of the normalized total pressure drop for the baseline concept is shown in Fig. 2.

Initially only three of the jets are supplied with fluid. These impinge within the cavity structure and then the flow splits as it exits. This spent flow from the primary impingement cavities then passes along internal channels to the three remaining jets. After the second impingement the fluid exits the structure through the central outlet channels.

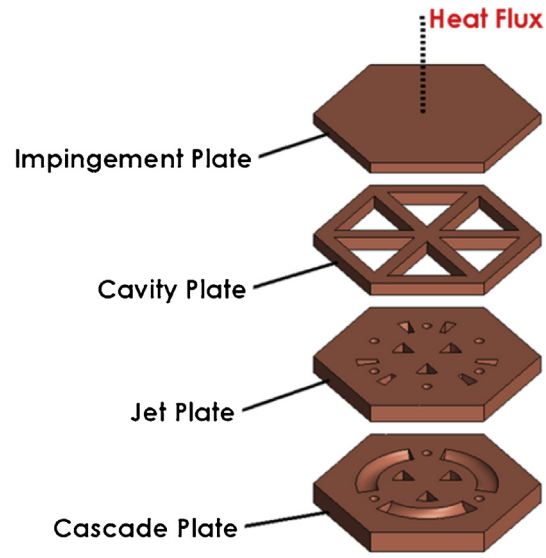

Fig. 3. Reference sheet composition and stacking order for baseline design.

This re-impinging of the same fluid element multiple times is called cascade impingement [6,7]. It is a system which enables additional pressure drop to be traded for a reduced mass flow rate.

Employing this method in the design is particularly effective due to the high operational pressure. As a result, multiple impingements can be performed before the total pressure drop becomes an appreciable percentage of the system pressure.

In Fig. 3 the four sheets composing the baseline design are shown, together with their stacking order.

Functionality of each of the laminate sheets in the final construction can be described as follows:

1. Impingement plate – withstand high incident heat fluxes normal to its surface.
2. Cavity plate – provide structural support to impingement plate for high system pressure.
3. Jet plate – provide inflow and outflow routes to cavities.
4. Cascade plate – provide multi-impingement flow-path and inlet and outlet routes to module.

Below the impingement plate it is important to try and minimize the rigidity of the structure to limit thermal stresses.

3. Thermo-fluid analysis

3.1. Methodology

Numerical simulations on the baseline geometry were performed using ANSYS 13.0 CFX. A conjugate model was employed in which it was assumed that the laminate structure could be treated as a single solid body.

A 120° periodic segment of the design was used for the simulations and meshed using ICEM. To accurately capture the gradients in the boundary layer 20 prism layers were grown to a height of 30 μm with a 1.25 growth ratio.

An incident heat flux of 10 MW/m^2 was applied to the impingement plate and all other external surfaces were assumed adiabatic. At the interface between the solid and fluid regions conservative heat influx was assumed.

At the fluid inlet the pressure was set to 20 MPa and the temperature to 150 °C. A mass flow rate was also prescribed and varied

Table 1
Numerical results for baseline design with fixed 300 °C area averaged wall temperature and 10 MW/m^2 incident heat flux.

ΔP [kPa]	ΔT_{fluid} [°C]	$\frac{\dot{m}}{A}$ [kg/m^2 s]	HTC [kW/m^2 K]	ΔT_{Surf} [°C]
159.0	38.8	60.4	86.1	31.7

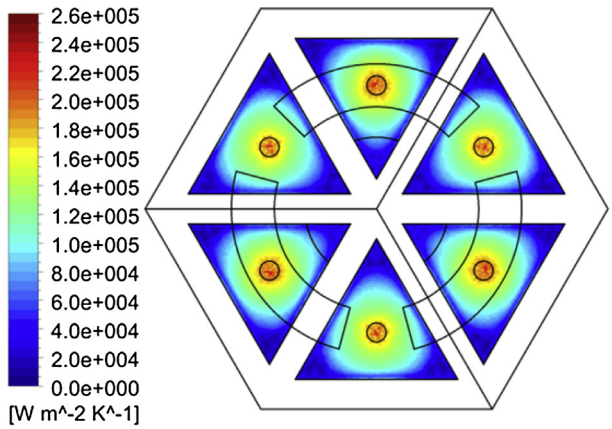

Fig. 4. Heat transfer coefficient in triangular cavities for baseline design.

until the area averaged temperature on the heat flux surface was 300 °C. At the outlet the area averaged pressure was set to 0 Pa.

Data for the CuCrZr was taken from [8,9] with an assumed conductivity of 83.4% IACS based on the ITER heat treatment. A neutron volume heating value of 10 MW/m^3 was also applied [10,11].

Water was modelled using the in-built IAPWS97 library in conjunction with the SST turbulence model. Turbulence numerics were set to second order and a specified blend factor of one used for the advection scheme.

3.2. Baseline case results

Quantitative values are given in Table 1 for the results of the simulation on the baseline geometry.

To achieve this area averaged wall temperature the maximum jet velocity was ~10.9 m/s and occurred in the secondary impingement nozzle. The associated peak heat transfer coefficient was ~260 kW/m^2 K.

Local variations in the heat transfer coefficient on the impingement surface are shown in Fig. 4.

Here the heat transfer coefficient has been defined as:

$$h = \frac{q'}{(T_{wall} - T_{jet})}$$

where q' is the wall heat flux, T_{wall} the wall temperature and T_{jet} the average temperature in the jet nozzle.

The secondary impingement cavity has a peak heat transfer coefficient that is ~9.5% higher than the primary value. When the area averaged values are compared this difference reduces to ~3%. This disparity is driven primarily by the increasing jet temperature between the two cavities and its impact on the Reynolds number.

Fig. 5 depicts the temperature variation on the incident heat flux surface. The peak temperature difference across the plate is driven by the primary impingement stagnation region and the vertices of the hexagon. At these outer vertices the temperature is 316 °C whilst at the primary stagnation point this drops to 284 °C. Higher temperatures at these outer tips should be acceptable as their impact on the structural integrity will be minimal.

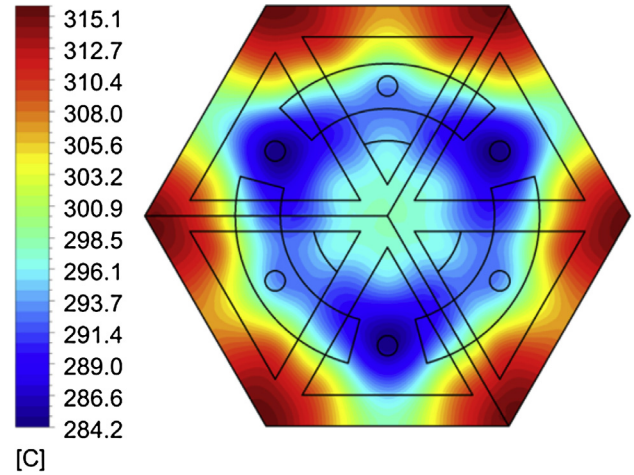

Fig. 5. Temperature distribution on incident heat flux surface for baseline geometry.

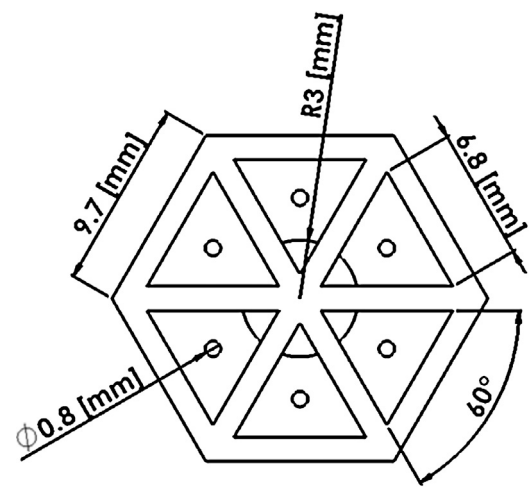

Fig. 6. Non-cascade geometry used for comparison.

3.3. Cascade comparison

Though the baseline geometry employs cascade impingement this is not a necessity for the design to function. To quantitatively compare a non-cascade system to the baseline design an additional set of simulations were performed on a 60° segment of the geometry depicted in Fig. 6.

No changes were made to the baseline geometry except to remove the cascade channels and alter the outlet locations for the primary impingement cavities. All other simulation parameters were the same as those described in Section 3.1.

Fig. 7 shows the ratio of the non-cascade system to the baseline case for a number of key thermo-fluid parameters.

Without cascading the system has a reduced pressure drop of 57.3 kPa. This is coupled with a mass flow rate per unit area increase to 115.9 kg/m^{2}s. Locally this implies that the jet Reynolds numbers of the cascade system are higher even though the mass flow rate per unit area is lower. The jets need to be driven at increased Reynolds numbers because the average bulk temperature of the fluid is higher in the cascade system.

Fig. 8 shows the heat transfer coefficient for the non-cascade system scaled against the peak value from the baseline case.

The area averaged heat transfer coefficient is ~4.9% smaller than the primary cavity from the baseline case. This is a result of the ~4.2% reduction in jet Reynolds number.

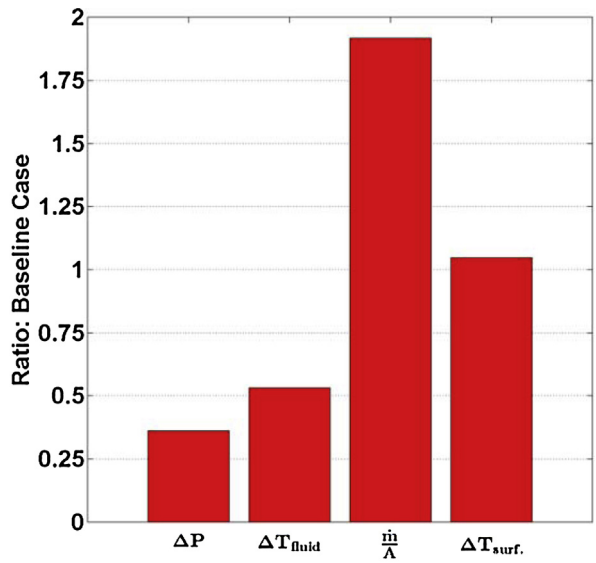

Fig. 7. Ratio of non-cascade system to baseline case for key thermo-fluid parameters.

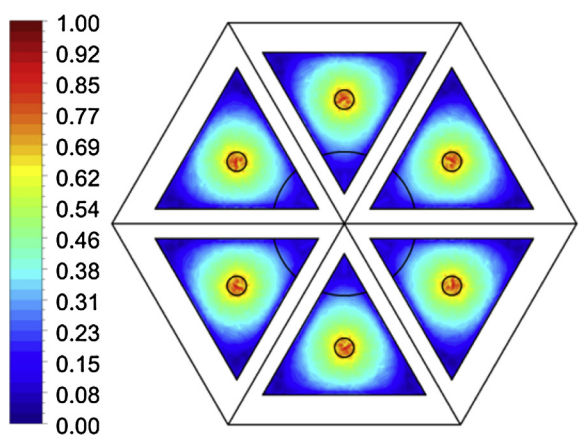

Fig. 8. Heat transfer coefficient in non-cascade system scaled against the peak value from the baseline case.

A potential drawback to cascading is the fact that the increasing bulk temperature may lead to higher temperature variations on the incident heat flux surface. This claim is investigated further in Fig. 9 where the following variable has been plotted:

$$T_{norm.} = \frac{T - T_{min}}{\Delta T_{surf}}$$

The value for the denominator here has been taken from the baseline case and T_{min} is the minimum temperature on the incident heat flux surface for the non-cascade design.

As with the cascade system the peak temperature difference is driven by the jet stagnation point and the hexagonal vertices. The peak at the vertices is slightly increased for the non-cascade system to a value of 319 °C compared to the 315 °C for the baseline case. This leads to the surprising result that cascading in this case reduces the surface temperature variation.

For a mass flow rate limited system cascading offers the potential to achieve much higher heat transfer coefficients than the traditional non-cascade geometry.

There is also the possibility that as well as cascading locally within an individual module we could cascade globally across the divertor plate. This would offer a novel way to dovetail with the heat flux profile over the divertor plate and maximize the fluid temperature change. If CuCrZr is allowed to run at its peak temperature of 350 °C this type of system may offer a means of increasing the temperature of the blanket coolant to an acceptable level to avoid embrittlement of RAFM steels.

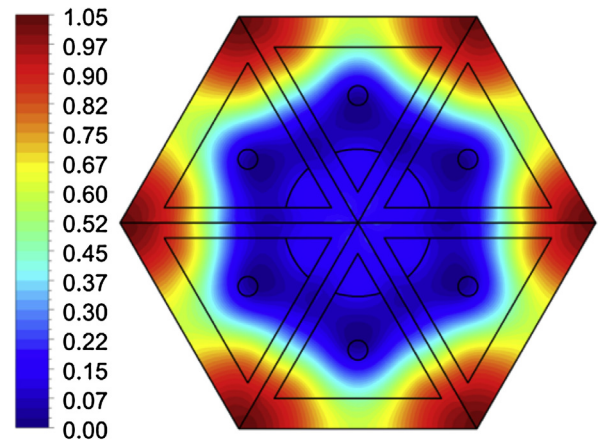

Fig. 9. Scaled temperature variation on the incident heat flux surface for the non-cascade system.

4. Experimental validation

4.1. Theory

To determine the validity of the numerical work experiments were carried out on the baseline design. Using air as the working fluid a 10× scale Perspex model was used to match similarity parameters.

The heat transfer coefficients were obtained by measuring the surface temperature response on the impingement plate to a step change in driving gas temperature. By assuming a semi-infinite substrate and 1D conduction this process can be modelled using the 1D Fourier equation.

To obtain local temperature data over the cavity narrow band thermochromic liquid crystals were used. As these crystals pass through their optically active phase their chiral pitch alters. This results in a change in the reflective properties of the crystal which can be measured using a light source and video camera. The optically active phase occurs at a particular temperature and because of this the local temperature over the surface can be recorded through time.

A numerical code developed in MATLAB by [12] is used to translate the time history of the temperature profile over the plate together with the driving gas temperature to determine the heat transfer coefficient.

4.2. Experimental apparatus

Each primary impingement cavity is fed by its own inlet channel. These each receive flow from a regulated 100 psi line. Within each of these inlet channels an orifice plate is used to measure the flow rate.

To achieve the step change in driving gas temperature an electrically heated mesh in the inlet flow channel is employed. These are linked in series and powered by a 600 W DC inverter.

Rubber seals are placed between the laminate sheets and the whole stack is pinned together using bolts at the hexagonal vertices. The outflow is fed through a circular channel and vented to atmosphere.

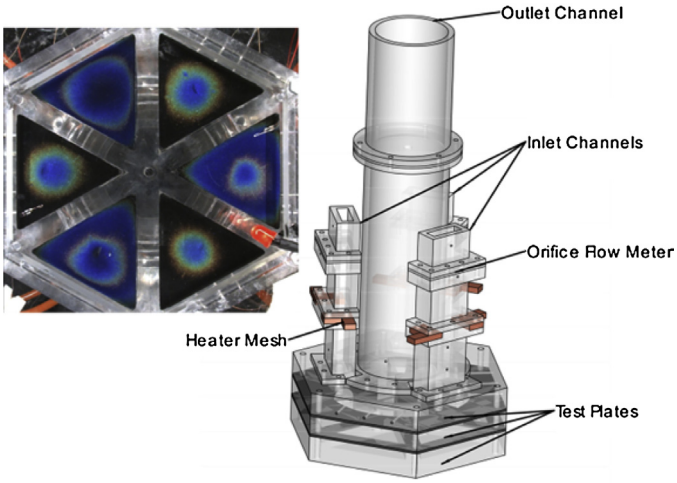

Fig. 10. Test section of experimental apparatus showing hexagonal plate together within inlet and outlet feeds [right]. Impingement plate during experimental run with liquid crystals [left].

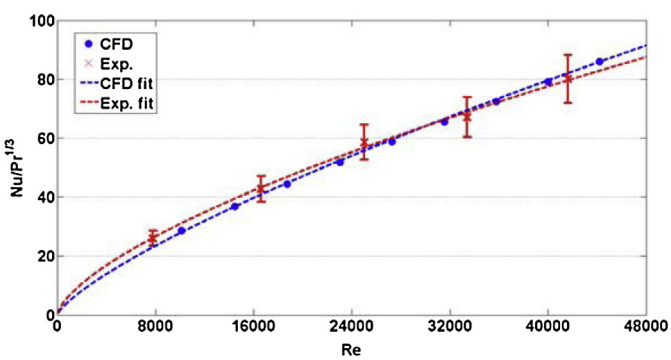

Fig. 11. Comparison of experimental and CFD results for scaled Nusselt number against Reynolds number.

The test section of the apparatus is shown in Fig. 10 together with a typical image of the impingement plate during a test run.

Video of the impingement plate is captured using a Point Grey Blackfly PGE-13E4C-CS at 32 Hz. For temperature readings k-type thermocouples were employed with a sample rate of 40 Hz.

4.3. Results and discussion

As different fluids have been employed for the numerical and experimental work Nusselt numbers are scaled using the Chilton-Colburn analogy [13].

In Fig. 11 the area averaged scaled Nusselt number in the primary cavity is plotted against Reynolds number for the experimental and numerical results.

Agreement to within experimental uncertainty is observed for all Reynolds numbers. This implies that the numerical methods employed are at least accurate in obtaining an area averaged value of the heat transfer coefficient for the Reynolds number range of interest.

Discrepancies may still exist between the two sets of results locally. To establish the validity of this claim we look at local data along the line from the central vertex of the triangle passing through the jet centre-line. This is shown in Fig. 12 with the scaled Nusselt number normalized against the value in the stagnation region.

There is close agreement in the form of the distribution between the numerical and experimental results. The observed offset between the two is driven by the large peak in the stagnation region of the numerical results. As there is close matching of the average values despite this behaviour it implies that the peak heat transfer coefficients must be smaller than those predicted by the numerical work. This result is advantageous for the design as it indicates that the actual heat transfer distribution is not as localized as the numerical results indicate. As a consequence, the temperature distribution on the impingement plate surface should be more uniform.

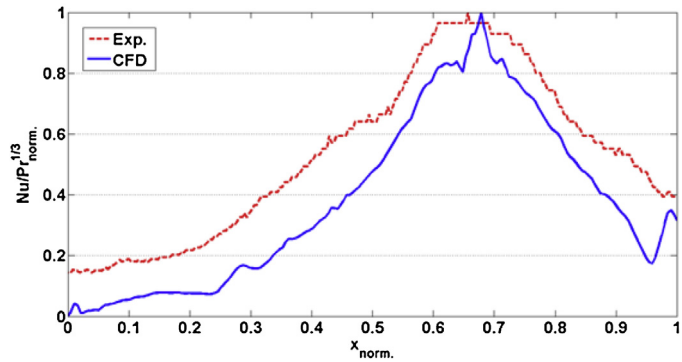

Fig. 12. Normalized scaled Nusselt number along jet centre-line through triangular cavity.

5. Conclusion and future work

A heat sink concept employing cascade jet-impingement for high-heat flux cooling applications has been introduced and developed.

The structure is composed of a number of CuCrZr sheets that are individually machined and then bonded together to form a laminate structure. This construction offers the possibility of building complex fluid flow paths without compromising on manufacturability.

To try and maximize the thermal efficiency of the power plant pressures of at least 16.5 MPa should be employed in the divertor. Above this pressure the saturation temperature of water is greater than the maximum operating temperature of CuCrZr.

A hexagonal profile was chosen for the laminate sheets to minimize thermal stresses and allow a tight packing of the divertor target plates. At the high operational pressures desired the scale of a single hexagon would have been impractical from a manufacturing point of view. To negate this issue the surface was divided into a number of triangular cavities.

A baseline geometry employing cascading was evaluated using ANSYS 13.0 CFX with an incident heat flux of 10 MW/m^2. This was compared to a non-cascade geometry that was otherwise equivalent. The results showed that for equivalent mass flow rates per unit area the cascade system produces higher heat transfer coefficients. An additional benefit of the reduced mass flow rate was that the overall temperature change of the fluid in the cascade system was also higher. Concerns for increased temperature variation on the heat flux surface using a cascade system were also shown to be unfounded.

To validate the numerical data a number of experimental measurements were performed on a scaled version of the model using air as the working fluid. Good agreement was found globally over the triangular cavity between the two sets of results. On a local level the numerical results were found to incorrectly predict the form of the distribution in the jet stagnation region. Outside of this zone the form of the distribution was similar between both.

Future work will look at the stress aspects of the design and aim to determine some of the key drivers in performance through an optimization study.

Acknowledgements

The author gratefully acknowledges the support of the EPSRC, CCFE and Rolls-Royce as funders for this research.

References

[1] T. Ihli, R. Kruessmann, I. Ovchinnikov, P. Norajitra, V. Kuznetsov, R. Giniyatulin, An advanced He-cooled divertor concept: design, cooling technology, and thermohydraulic analyses with CFD, Fusion Eng. Des. 75–79 (2005) 371–375.
[2] P. Norajitra, A. Gervash, R. Giniyatulin, T. Hirai, G. Janeschitz, W. Krauss, et al., Helium-cooled divertor for DEMO: manufacture and high heat flux tests of tungsten-based mock-ups, J. Nucl. Mater. 386–388 (2009) 813–816.
[3] J. Reiser, M. Rieth, Optimization and limitations of known DEMO divertor concepts, Fusion Eng. Des. 87 (2012) 718–721.
[4] M.S. Tillack, A.R. Raffray, X. Wang, S. Malang, Recent US activities on advanced He-cooled W-alloy divertor concepts for fusion power plants, Fusion Eng. Des. 86 (2010) 71–98.
[5] D. Stork, P. Agostini, J.L. Boutard, D. Buckthorpe, E. Diegele, S.L. Dudarev, et al., Developing structural, high-heat flux and plasma facing materials for a near-term DEMO fusion power plant: the EU assessment, J. Nucl. Mater. 455 (2014) 277–291.
[6] B. Cheong, P.T. Ireland, A. Siebert, A cooling arrangement, Application WO2005117108 A1, May 25 (2004).
[7] M. Kopmels, M.T. Mitchell, P.J. Goodman, K.C. Sadler, Air-cooled component, Grant US7976277 B2, November 9 (2006).
[8] S.J. Zinkle, W.S. Eatherly, Effect of heat treatments on the tensile and electrical properties of high-strength, high-conductivity copper alloys, Oak Ridge National Laboratory.
[9] M. Li, J.S. Zinkle, Physical and mechanical properties of copper and copper alloys, Compr. Nucl. Mater. 4 (2012) 667–690.
[10] Y. Ikeda, F. Maekawa, M. Wada, Y. Kasugai, C. Konno, Y. Uno, et al., Nuclear Heating Measurements for SS-316, copper, Graphite, Tungsten, Chromium, Beryllium in a copper Centred Assembly Bombarded with 14 MeV Neutrons and Analysis, vol. 42, 1998, pp. 289–297.
[11] A. Kumar, M.Z. Youssef, M.A. Abdou, Direct Nuclear Heating Measurements in Fusion Neutron Environment and Analysis, vol. 18, 1991, pp. 397–405.
[12] M. McGilvary, D. Gillespie, Transient Heat Transfer Analysis Code for Liquid Crystal Experiments at the University of Oxford: Updated GUI Driven Software, University of Oxford, Oxford, 2011 (manual).
[13] F.P. Incropera, D.P. DeWitt, in: V.A. Vargas (Ed.), Fundamentals of Heat and Mass Transfer, 6th ed., John Wiley & Sons, United States, 2006.